IOPscience iopscience.iop.org

Selective area *in situ* conversion of Si (0 0 1) hydrophobic to hydrophilic surface by excimer laser irradiation in hydrogen peroxide

This content has been downloaded from IOPscience. Please scroll down to see the full text.

View the table of contents for this issue, or go to the journal homepage for more

Download details:
This content was downloaded by: dubj2003
IP Address: 132.210.83.216
This content was downloaded on 29/09/2014 at 00:23

Please note that terms and conditions apply.

2014 J. Phys. D: Appl. Phys. 47 385106

IOP Publishing Journal of Physics D: Applied Physics
J. Phys. D: Appl. Phys. **47** (2014) 385106 (9pp) doi:10.1088/0022-3727/47/38/385106

Selective area *in situ* conversion of Si (0 0 1) hydrophobic to hydrophilic surface by excimer laser irradiation in hydrogen peroxide

Neng Liu, Xiaohuan Huang and Jan J Dubowski

Laboratory for Quantum Semiconductors and Photon-based BioNanotechnology, Interdisciplinary Institute for technological Innovation (3iT), Laboratoire Nanotechnologies Nanosystèmes (LN2)- CNRS UMI-3463, Faculty of Engineering, Université de Sherbrooke, Québec J1K 2R1, Canada

E-mail: jan.j.dubowski@usherbrooke.ca

Received 7 April 2014, revised 21 July 2014
Accepted for publication 1 August 2014
Published 28 August 2014

Abstract

We report on a method of rapid conversion of a hydrophobic to hydrophilic state of an Si (0 0 1) surface irradiated with a relatively low number of pulses of an excimer laser. Hydrophilic Si (0 0 1), characterized by the surface contact angle (CA) of near 15°, is fabricated following irradiation with either KrF or ArF excimer lasers of hydrophobic samples (CA ∼ 75°) immersed in a 0.01% H_2O_2/H_2O solution. The chemical and structural analysis carried with x-ray photoelectron spectroscopy and atomic force microscopy measurements confirmed the formation of OH-terminated Si (0 0 1) surface with no detectable change in the surface morphology of the laser-irradiated material. To investigate the efficiency of this laser-induced hydrophilization process, we demonstrate a selective area immobilization of biotin-conjugated fluorescein-stained nanospheres outside of the laser-irradiated area. The results demonstrate the potential of the method for the fabrication of biosensing architectures and advancements of the Si-based microfluidic device technology.

Keywords: silicon, surface wettability, laser–surface interaction, selective area processing, hydrophobic to hydrophilic transition, x-ray photoelectron spectroscopy

(Some figures may appear in colour only in the online journal)

1. Introduction

The remarkable electronic properties and high mechanical strength have made silicon (Si) an attractive choice for applications involving microfluidic technology and biochip fabrication (Guo *et al* 2013, Li *et al* 2007). The wettability of Si in such applications is one of the key parameters important to control attachment and/or displacement of molecules (Daniel *et al* 2001, Bayiati *et al* 2007). Typically, strongly hydrophobic surfaces have been obtained by modification of Si surface morphology involving nanostructure fabrication (Li *et al* 2007, Cho *et al* 2011), while hydrophilic surfaces have been obtained by modification of Si both surface roughness and chemistry (Sun *et al* 2008). The structuring to produce a variety of wetting-controlled microstructures on the Si surface includes photolithography (Krupenkin *et al* 2004), ion-beam lithography (Martines *et al* 2005) and laser techniques (Baldacchini *et al* 2006, Ranella *et al* 2010). In comparison with conventional techniques, laser surface micro/nanostructuring is a direct (mask-free) approach. Thus, it has the potential to offer design flexibility as well as economically attractive solutions (Zorba *et al* 2006). However, as Si has a relatively high texturing threshold of ∼500 mJ cm^{-2} (Tsu *et al* 1991), the low-damage micro/nanostructuring of this material requires the assistance of reactive gases, such as SF_6 (Zorba *et al* 2006, Sun *et al* 2008, Ranella *et al* 2010). Numerous works addressing wettability of Si have employed lasers to induce or assist modification of the Si surface chemical

 © 2014 IOP Publishing Ltd Printed in the UK

composition by depositing organic or metal oxide films on the surface before laser irradiation (Li *et al* 2007, Caputo *et al* 2008). For instance, a UV laser has been successfully applied to irradiate TiO_2-coated Si and generate oxygen vacancies with affinity to water, resulting in the surface contact angle (CA) of near 10° (Caputo *et al* 2008). It is known that hydrophilicity of Si originating from the presence of singular and associated OH groups on its surface could be obtained by boiling it in an H_2O_2 solution at 100 °C for several minutes (Bal *et al* 2010b). In contrast, the hydrophobic Si surface state, mainly characterized by Si–H or Si–O–CH_3 groups, could be obtained by wet chemical treatment involving HF acid or photoresists (Grundner and Jacob 1986, Bal *et al* 2010a, 2010b). UV lasers have also been used to induce chemical or thermal dissociation and adsorption of different gases (methanol, water vapour, etc) on the Si surface (Koehler *et al* 1989, Tanaka *et al* 1993). However, a limited volume of work has been devoted to the study of the chemical modification of the Si surface in the context of surface wettability of this material. X-ray photoelectron spectroscopy (XPS) measurements have shown that both C/Si and O/Si ratios of an air exposed Si (1 0 0) decrease after KrF laser irradiation in air, illustrating the so-called 'laser cleaning effect' (Tsu *et al* 1991). At the same time, as the C content decreased with the pulse number, CA was found decreasing from 75° to near 52°, similarly to the effect of coating Si with thermal oxide (Tsu *et al* 1991). In our previous work, UV laser was successfully used to modify surface chemical composition of GaAs, InGaAs and InP irradiated in air (Dubowski *et al* 1999, Genest *et al* 2007, Genest *et al* 2008) and NH_3 (Wrobel *et al* 1998). We found that UV laser irradiation of InP in deionized (DI) water reduces the presence of surface oxides and carbides, while it enhances adsorption of water on the surface of a semiconductor (Liu *et al* 2013). Following these observations, we have employed an ArF laser for the irradiation of Si samples immersed in methanol and we have demonstrated the formation of strongly hydrophobic surfaces (CA $\sim$ 103°), primarily due to the ability of the ArF laser to induce photo-dissociation of CH_3OH (Liu *et al* 2014).

Here, we report on the KrF and ArF excimer laser-induced modification of the hydrophobic state of Si (0 0 1) samples immersed in a low concentration of H_2O_2 solution with the purpose of selective area formation of a strongly hydrophilic surface.

2. Experimental details

One-side polished, 3 inch diameter, 380 μm thick n-type (P-doped) Si (1 0 0) wafers (resistivity 3.1–4.8 Ω m) were employed in this study. Small coupons of 12 mm × 6 mm were cleaved from the wafer. The coupons were first cleaned with Opticlear, acetone and isopropyl alcohol, each for 5 min, then they were lightly etched in a diluted 1 : 50 HF (48%) (Anachemia Science) solution for 1 min to remove the native oxide (Mizuno *et al* 1991). Following the etching step, the samples were rinsed with DI water and dried with high-purity (99.999%) nitrogen. The samples were placed in a 0.74 mm tall chamber that was sealed with a fused silica window transmitting more than 90% of UV radiation. The chamber was filled with water diluted H_2O_2 (Fisher Scientific) in the range 0.01–0.2%. The samples were irradiated with KrF (λ = 248 nm) and ArF (λ = 193 nm) lasers (Lumonics, Pulse master 800) operating at 2 Hz. For each laser pulse fluence, only two sites were irradiated on each coupon with 100/200, 300/400 or with 500/600 pulses. A double micro-lens fly-eye-array was used to generate a beam of the uniform intensity (σ_{RMS} = 5%) over the area of 15 mm × 11 mm. A circular mask of a 4 mm diameter or a 9 mm × 7.2 mm 'maple leaf' mask was installed at the centre of the homogenized field and projected on the sample surface at the demagnification ratios of 1.8 (KrF laser) or 2.6 (ArF laser). With a computer controlled *X*–*Y*–*Z*–theta positioning of the sample, the whole beam shaping and delivery setup (MBX JPSA Sercel, Manchester, NH) allowed for precise changing of the sample position and carrying out irradiation of numerous sites. Following the laser irradiation, samples were rinsed with DI water, dried with nitrogen and installed in a sealed nitrogen container to limit their exposure to an atmospheric environment before further surface characterization experiments.

Static CA measurements were carried out with a goniometer (Rame-Hart NRL, Model 100) at room temperature and ambient humidity. High-purity deionized water with electrical resistivity typically of 17.95 MΩ cm was employed to generate drops, each approximately of 5 μl in volume. The profile images of sessile water drops on the samples were captured by CCD camera (Logitech). Four independent measurements were performed on different sites irradiated nominally under the same conditions. The analysis of the drop images was carried out with the VP-eye 6.0 software (MMedia) and the CA values were determined by the drop analysis with the ImageJ software.

Excimer laser-induced surface chemical modification was investigated with a 1 × 10^{-9} Torr base pressure XPS spectrometer (Kratos Analytical, AXIS Ultra DLD) equipped with an Al Kα source operating at 150 W. The surface survey and high-resolution scans were observed in constant energy modes at 50 eV and 20 eV pass energy, respectively. The size of an analysed area on the investigated samples was set at 220 μm × 220 μm. The XPS spectra were processed using the Casa XPS 2.3.15 software. To compensate the surface charging effect, all XPS data were referenced to the adventitious C 1s peak at the binding energy (BE) of 285.0 eV (Mizuno *et al* 1991, Swift and Cramb 2008). Two Lorentzian asymmetric line shape peaks were applied to Si 2p, including Si 2p 3/2 and Si 2p 1/2 spin states with equal FWHM. The area ratio and energy separation of Si 2p 1/2 to Si 2p 3/2 was taken as 0.5 and 0.61 eV, respectively (Grunthaner *et al* 1987).

Fourier transform infrared spectroscopy (FTIR) data were collected with a Bruker Optics Vertex80 spectrometer operating under ambient conditions. The signal was collected and focused on a liquid N_2 cooled HgCdTe broadband detector with a resolution of 4 cm^{-1}. The analysed area was approximately 3 mm in diameter.

Upon irradiation through a 'maple leaf' mask and washing with DI water, the samples were immersed for 2 h in a pH 7.4 phosphate buffered saline (PBS, 1X) solution (Sigma,

Canada) of biotin-conjugated and fluorescein-stained 40 nm diameter nanospheres (Invitrogen, Burlington, Canada). This step was followed by washing the sample with PBS to remove nanospheres weakly bound to the surface. The laser fabricated hydrophilic surface of Si was expected to prevent the nanospheres from immobilization, as the biotin protein is hydrophobic in nature (Swift and Cramb 2008). The fluorescence was excited with a blue light source emitting between 450 and 490 nm. The fluorescent images were observed at 515 nm using a fluorescence inverted microscope (Olympus, IX71) equipped with a DP71 digital camera. Surface morphology of samples, after laser irradiation and functionalized with biotin-conjugated nanospheres, was imaged with AFM (Digital Instrument, Nanoscope III) operating in a tapping mode. The AFM images were collected over the 5 μm × 5 μm region with 512 points per line at a rate of 1.97 Hz, allowing for high accuracy roughness measurement and surface morphology imaging (Liu *et al* 2012).

3. Results and discussion

3.1. CA measurements

Figure 1 demonstrates the CA dependence on pulse number for sites irradiated in DI water and 0.01, 0.02, 0.05 and 0.2% H_2O_2 solutions using a KrF laser at 250 mJ cm^{-2}. The insets show examples of profile images of water drops on (*a*) non-irradiated sample (CA = 75°) and on (*b*) sites irradiated with 200 pulses (CA = 38°) and (*c*) 500 pulses (CA = 15°) of samples immersed in the 0.01% H_2O_2 solution. We can see that the CA decreases as the pulse number increases for all the H_2O_2 solutions. The CA for 0.02% and 0.01% H_2O_2 solutions decreased to 15° at 500 pulses. Somewhat greater CA has been observed for 0.05% and 0.2% H_2O_2 solutions. At the same time, CA of the non-irradiated material ($N = 0$) decreased from 75° to 43° as the H_2O_2 concentration increased from 0.02% to 0.2%. In a series of experiments, we have observed that a room-temperature spontaneous reaction in 0.01% H_2O_2 leads to CA decreased by less than 10°, mostly within the first 3–4 h of the exposure. Thus, in the process of decreasing CA by 60° (from 75°) within a ~4 min exposure to the KrF laser (250 mJ cm^{-2}) operating at 2 Hz, the spontaneous reaction plays a negligible role.

The results for the non-irradiated material in figure 1 were obtained after an average 10 min exposure to H_2O_2 solutions and they represent the CA values near the saturation obtainable at respective H_2O_2 concentrations. Note that hydrophilic OH-terminated Si surfaces, with CA near 10°–15° and ~25°, have been fabricated by boiling Si samples at 100 °C for 10 min in solutions of H_2O : NH_4OH : 30% H_2O_2 = 2 : 1 : 1 and H_2O : HCl : 30% H_2O_2 = 1 : 1 : 6, respectively (Bal *et al* 2010b, Hermansson *et al* 1991). Our results indicate that the short-time exposure of Si to a 0.01% H_2O_2 solution alone has not been able to induce a significant change to its CA. Furthermore, as shown in figure 1, CA of the sites irradiated in DI water shows no obvious change for the pulse number as large as 600. Some increase in CA has been observed for $N > 300$ pulses in 0.2% and 0.05% solutions, and for $N > 500$ pulses in 0.02%

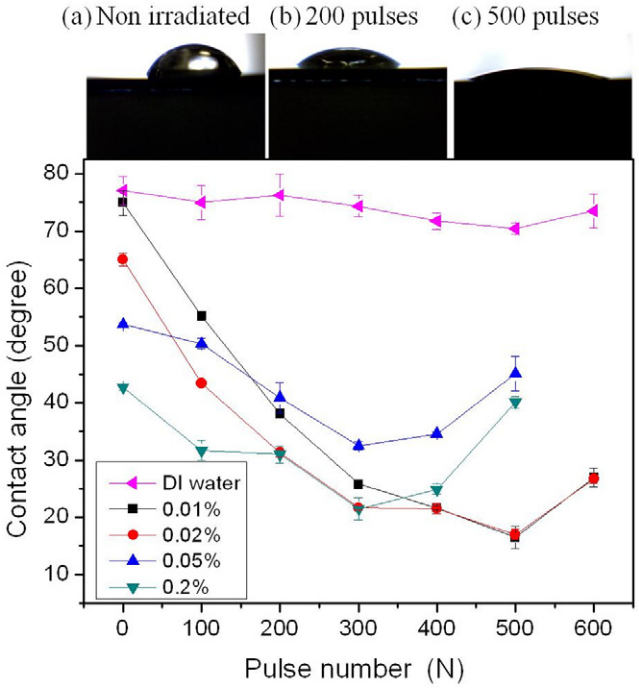

Figure 1. CA versus pulse number of KrF laser-irradiated Si (0 0 1) at 250 mJ cm^{-2} in DI water, and in 0.01%, 0.02%, 0.05% and 0.2% H_2O_2/DI water solutions. Experimental points are indicated by the respective symbols and the solid lines have been included as a guide to the eye. The insets show profile images of water drops on (*a*) non-irradiated Si with CA = 75° and sites irradiated with (*b*) 200 pulses (CA = 38°) and (*c*) 500 pulses (CA = 15°) by the KrF laser in a 0.01% H_2O_2/DI water solution.

and 0.01% solutions, indicating that the reversal of the CA decreasing trend occurs more rapidly in greater concentrations of H_2O_2. A possible reason for this behaviour could be a laser-accelerated decomposition of H_2O_2 ($2H_2O_2 \rightarrow 2H_2O+O_2$) at a rate that is known to increase with the increasing concentration of H_2O_2 (Croiset *et al* 1997). Furthermore, the hydrophilicity inducing Si–OH groups observed on the surface of laser-irradiated samples (as discussed further in this paper), after reaching a critical density could begin to condense (Gräf *et al* 1989) and decrease the hydrophilic nature of the investigated samples.

In figure 2, we compare the CA dependence on pulse number for the sites irradiated in a 0.01% H_2O_2 solution using KrF (figure 2(*a*)) and ArF (figure (*b*)) lasers. The overall tendency of CA to decrease with the irradiation pulse number is observed for up to 600 pulses of the KrF and ArF lasers operating at 183 mJ cm^{-2} and 44 mJ cm^{-2}, respectively. The minimum CA of ~15° has been achieved with 300 and 500 pulses of the KrF laser operating at 320 mJ cm^{-2} and 250 mJ cm^{-2}, respectively. The same CA ~15° has also been obtained with 500 pulses of the ArF laser operating at 65 mJ cm^{-2}. These results seem to point out to the laser-induced surface temperature as the leading process responsible for the production of OH and hydrophilization of Si in an H_2O_2/H_2O environment. Using COMSOL calculations, based on Si parameters listed in table 1, we have estimated that the surface peak temperature induced with 250 mJ cm^{-2} and 320 mJ cm^{-2} pulses of the KrF laser is 88 °C and

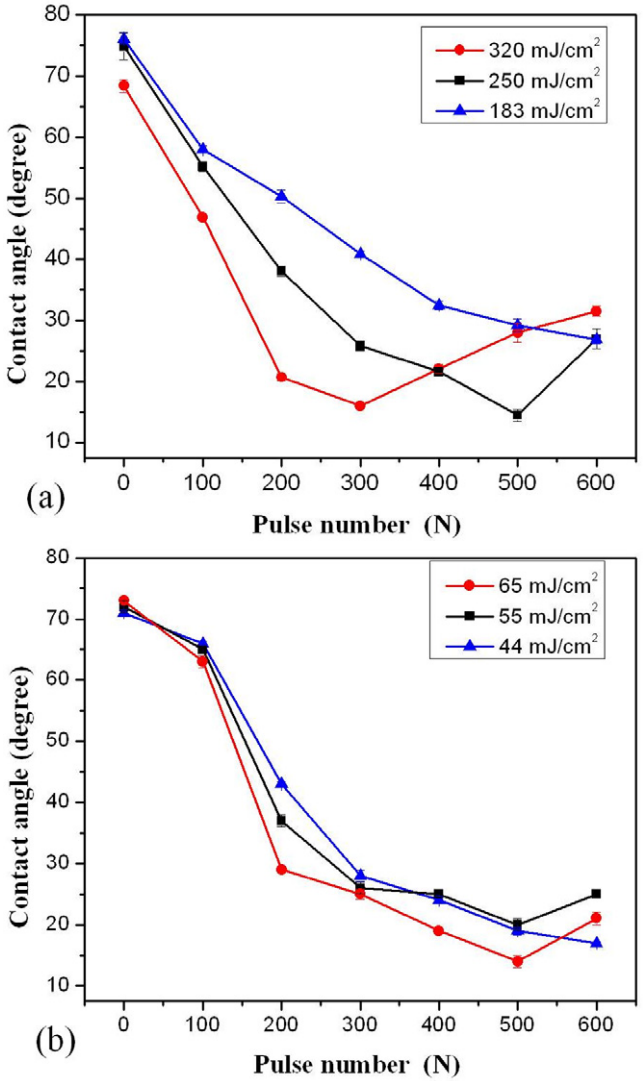

Figure 2. CA versus pulse number after irradiation in a 0.01% H_2O_2 solution with KrF (*a*) and ArF (*b*) lasers of different pulse fluences.

95 °C, respectively. These compare with 40 °C of the peak temperature induced with a 65 mJ cm^{-2} pulse of the ArF laser. In the calculations, we assumed that the optical absorption (α) of H_2O_2/H_2O solutions is comparable to that of DI H_2O at 196 and 248 nm, i.e. 126×10^{-2} m^{-1} and 3.92×10^{-2} m^{-1}, respectively (Quickenden and Irvin 1980). This is a reasonable assumption given the low H_2O_2 concentration (0.01–0.2%) in the investigated solutions.

The calculations have indicated that the peak temperature of 88 °C decreases to 32 °C in approximately 10^{-5} s from the laser pulse onset. Thus, with the pulse repetition rate of 2 Hz it is unlikely to increase significantly the sample temperature through the accumulative process. The situation is slightly different, however, for KrF laser pulses of 320 mJ cm^{-2}.

The ability of the KrF laser pulse fluence of 320 mJ cm^{-2} to induce the surface temperature near the boiling point of H_2O coincides with our observation of a large concentration of bubbles formed in this case at the sample–liquid interface, especially for large pulse number. The accumulative effect of the laser-induced heating of the Si–liquid interface has also been observed for the portion of the coupon that remained non-irradiated during this experiment. As shown in figure 2(*a*), the CA value of a material at N =0 has decreased from 75° to 69°, suggesting the presence of a temperature-enhanced hydrophilization process. Consistent with the less efficient heating of Si at reduced pulse fluence was the observation that CA of 75°, characterizing the HF-etched material, was not significantly affected by the accumulative (indirect) heating of coupons irradiated with pulses at 183 and 250 mJ cm^{-2}. The effect of the reversal of the CA trend is observed in this case for 250 mJ cm^{-2} ($N > 500$ pulses) and 320 mJ cm^{-2} ($N > 300$ pulses), which is consistent with the suggested effect of the laser-accelerated decomposition of H_2O_2 and/or condensation of the Si–OH groups. Note that the loss of OH in the sample reservoir could be compensated by working with a continuously refreshing flow of H_2O_2/H_2O as opposed to the closed volume employed in this experiment. Generally, the formation of bubbles made it difficult to collect a reliable set of data for $N > 400$ and 600 and pulse fluence of 320 mJ cm^{-2} and 250 mJ cm^{-2}, respectively.

Table 1. Parameters of Si used in the calculation of spatial and transient temperature profiles.

Thermal conductivity	Specific heat	Density	Optical absorption
34 (W m^{-1} K^{-1}) (Glassbrenner and Slack 1964)	678 (J kg^{-1} K^{-1}) (Flubacher *et al* 1959)	2320 (kg m^{-3}) (Lukeš and Černý 1992)	1.64×10^8 (m^{-1}) (Aspnes and Studna 1983)

For the ArF laser, the smallest CA value of ∼15° was achieved with 500 pulses of the 65 mJ cm^{-2} pulse fluence. As the surface peak temperature induced in this case is only 40 °C, it seems that the formation of a hydrophilic surface has been affected by enhanced photo-dissociation of H_2O_2 that produces OH group required for the hydrophilization of the investigated samples. It is important to note that H_2O_2 absorption at 193 nm is 7× stronger than at 248 nm (Schiffman *et al* 1993). This process could be further enhanced by the laser heating of water that absorbs approximately 32× stronger at 196 nm ($\alpha = 126 \times 10^{-2}$ m^{-1}) than at 248 nm ($\alpha = 3.92 \times 10^{-2}$ m^{-1}) (Quickenden and Irvin 1980). The net result of enhanced photo-dissociation would be an increased concentration of OH radicals available for the reaction with Si and its hydrophilization. We found it impractical to irradiate the samples with ArF laser at the fluence exceeding 65 mJ cm^{-2} due to the formation of a large number of bubbles increasing in proportion to the number of laser pulses delivered to the surface.

3.2. AFM analysis

Surface morphology of Si samples was investigated to address the possible modification of CA due to the increased surface roughness (Zorba *et al* 2006). Figure 3 shows an AFM image of (*a*) a fragment of the HF-etched sample that was not laser irradiated, but remained in the 0.01% H_2O_2/H_2O solution for approximately 10 min during laser processing, and (*b*) a site on

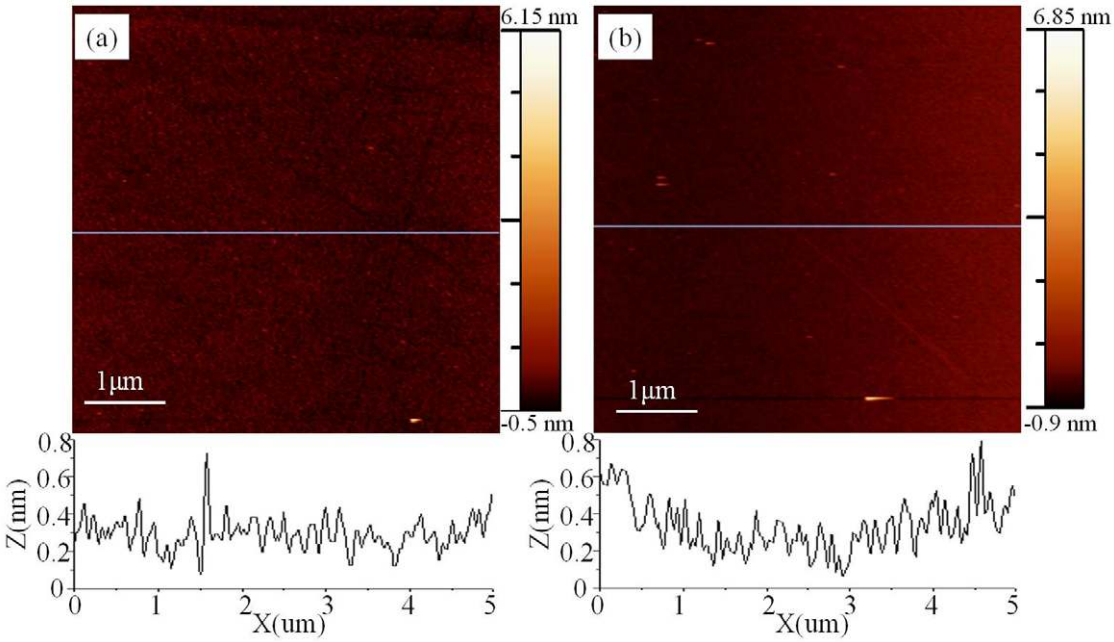

Figure 3. AFM images of a non-irradiated sample (*a*) and a site irradiated with KrF laser at 250 mJ cm^{-2} with 500 pulses (*b*) of the sample kept for ∼10 min in a 0.01% H_2O_2/H_2O solution.

the same sample irradiated with 500 pulses of the KrF laser at 250 mJ cm^{-2}. We found that the roughness (σ_{RMS}) of the non-irradiated material and that of the irradiated site is 0.30 nm and 0.38 nm, respectively. This indicates that there is no obvious surface morphology modification during laser irradiation of Si samples immersed in the H_2O_2/H_2O solution.

3.3. XPS analysis

Figure 4 shows Si 2p and O 1s XPS spectra of a freshly HF-etched Si surface (4a, 4 d), non-irradiated Si surface exposed to 0.01% H_2O_2 solution for approximately 10 min (figures 4(*b*) and (*e*)), and Si sites exposed to 0.01% H_2O_2/H_2O solution and irradiated with 500 pulses of the KrF laser at 250 mJ cm^{-2} (figures 4(*c*), (*f*)). The Si 2p XPS spectra were fitted with Si, Si sub-oxides (SiO_x, $x < 2$), oxides (SiO_2) and silicon hydroxides (SiOH) (Grunthaner *et al* 1987). The Si 2p 3/2 of elemental Si was fixed at BE $= 99.2 \pm 0.1$ eV, while the peaks of SiO_x and SiO_2 were shifted by 0.7 eV and 3.8 eV, respectively (Grunthaner *et al* 1987). The OH replacing the oxygen atom has little impact on the Si 2p, so the SiO_2 and SiOH peaks were fixed at the same position in the Si 2p spectra (Heo and Kim 2007).

In comparison with the as-received material, HF etching significantly reduces the XPS concentration of oxygen originating from the surface present SiO_2 (data not shown). Consistent with this is the CA value of the as-received material, determined to be 51°, that increased to 75° following the etching procedure (see table 2). The 500-pulse irradiated sites exhibit significantly increased concentrations of both SiOH and SiO_2, consistent with the increased material hydrophilicity. In the O 1s spectra, the peaks at 531.8 ± 0.1 eV, 532.6 ± 0.1 eV and 533.7 ± 0.1 eV were assigned to SiO_x, SiO_2 and SiOH, respectively (Grunthaner *et al* 1987, Heo and Kim 2007). Since OH has a direct effect on the O 1s, a BE shift is observed between SiO_2 and SiOH in the O 1s spectra (Heo and Kim 2007). After etching in the HF solution, most of SiO_2 and SiO_x have been removed, as shown in figure 4(*d*). The quantity of SiO_2 and SiOH is greater for the irradiated site (figure 4(*f*)) than that for the non-irradiated material (figure 4(*e*)). Depending on the O/Si ratio, the minimum CA values of SiO_2-coated Si have been reported to be 45°–55° (Chasse and Ross 2002), while the minimum CA of 13° has been reported for a SiOH monolayer covered Si surface (Chen *et al* 1991). Thus, the increase in SiOH plays a dominating role in decreasing CA to 14° at 500 pulses. The XPS fitting of the O 1s spectra allowed one to determine that the $SiOH/SiO_2$ ratio increased from 0.10 to 0.17 when pulse number increased from 100 (not shown here) to 500. The formation of the Si–OH bond is possibly due to the availability of negatively charged OH radicals formed by the UV laser-induced photolysis of H_2O_2, as discussed in section 3.1. The interaction of OH radicals with Si is facilitated by the excimer laser-induced photoelectric effect, which leads to the formation of a positively charged Si surface (Chen *et al* 1988). The increased concentration of OH reacting with Si is expected to increase its hydrophilicity (Grundner and Jacob 1986). Furthermore, decomposition of thermodynamically unstable H_2O_2 could be accelerated by impurities (Rice and Reiff 1927, Averill and Eldredge 2007) and/or catalysts, such as iron oxides (Lin and Gurol 1998). It is feasible that similar decomposition channels are present in our experiment and lead to the formation of excessive O_2 in the vicinity of the Si surface. While the potentially important consequence of this process in achieving a hydrophilic surface of Si would be the formation of SiO_2, the presence of O_2 molecules could also be the source of bubbles forming near the irradiated surface. As discussed above, we have observed significantly

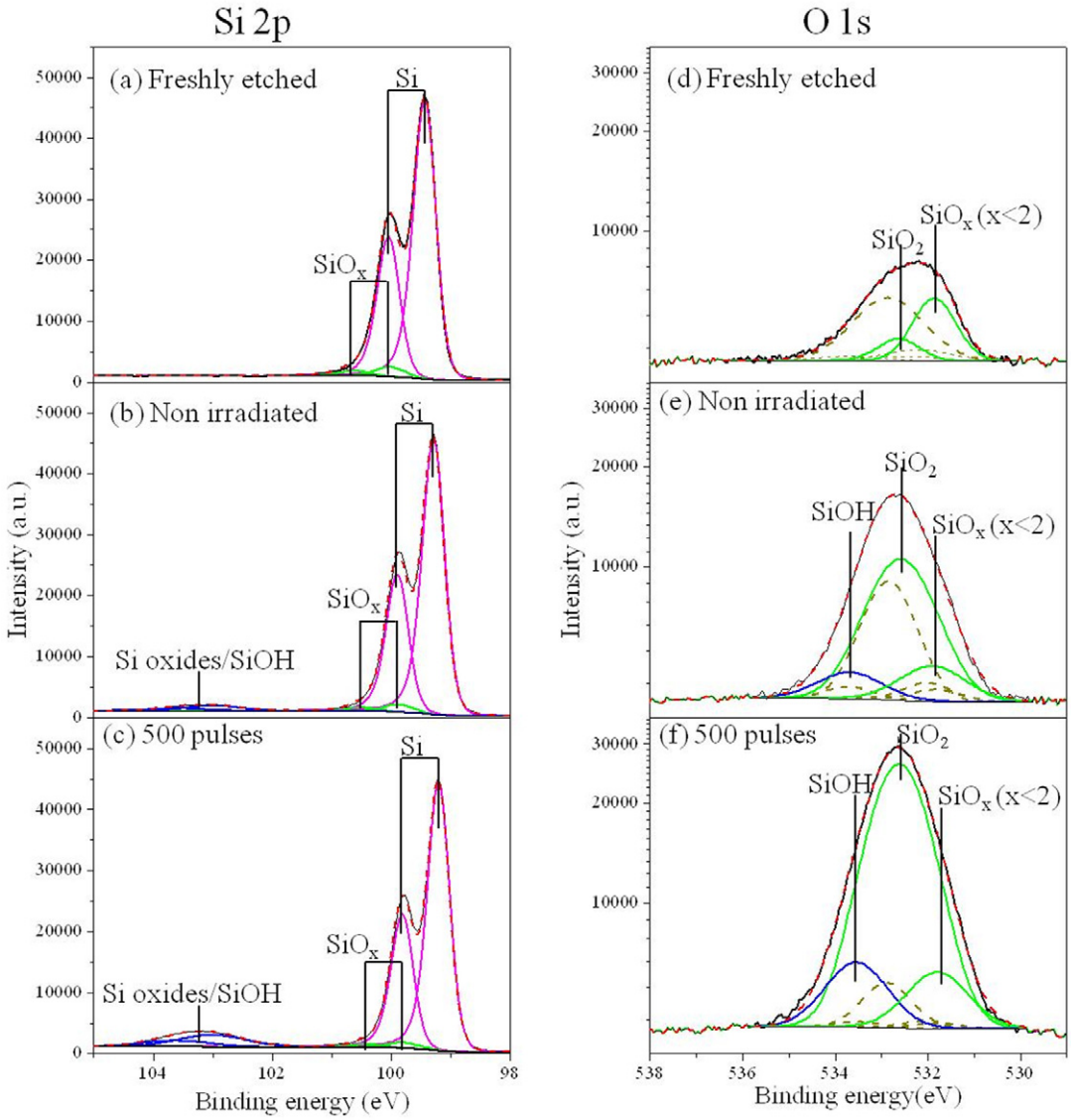

Figure 4. Si 2p and O 1s XPS spectra of a freshly etched site (*a*), (*d*), non-irradiated sample kept for 10 min in a 0.01% H_2O_2/H_2O solution (*b*), (*e*) and a site exposed to a 0.01% H_2O_2 solution and irradiated with 500 pulses of the KrF laser (*c*), (*f*).

increased bubble formation in experiments involving ArF laser at 65 mJ cm^{-2} and KrF laser at 320 mJ cm^{-2}, consistent with the increased possibility of thermally or photo-driven decomposition of H_2O_2. The increase in CA observed for the sites irradiated with a large pulse number could be related to the formation of SiO_2-enriched Si.

The dashed lines in the O 1s spectra correspond to carbon (C) adsorbates, whose quantities are calculated from the known ratios of oxygen to carbon in the C 1s spectra originating from C–O, C=O and O–C=O bonds (Miller *et al* 2002). It can be seen that the concentration of C is greater on the surface of a non-irradiated but exposed to the H_2O_2/H_2O solution material, than on the freshly etched sample. As shown in figure 4(*f*), the concentration of C absorbates is reduced with the increasing pulse number due to the known excimer laser cleaning effect (Tsu *et al* 1991). Since the C absorbates contribute to the hydrophobic nature of Si (Grundner and Jacob 1986), the laser-induced cleaning of the Si surface of the C adsorbates helps one to enhance the hydrophilic properties of the Si surface.

Table 2 shows atomic concentrations of Si, O, C, F and the CA values observed for as-received, etched and KrF laser irradiated at 250 mJ cm^{-2} samples. Due to the high coverage with native oxide (O/Si $\sim$ 1.4), CA of as-received material is 51°. As this oxide is removed by HF treatment, CA increased to 75°. Following the sample exposure to 0.01% H_2O_2 solution, the oxygen atomic percentage and the O/Si ratio increase with pulse number due to UV laser-induced formation of SiOH. Table 3 shows the values of atomic concentrations of Si, O, C, F and CA observed for as-received, etched and ArF laser-irradiated samples at 65 mJ cm^{-2} with 100 and 500 pulses. XPS fitting shows that $SiOH/SiO_2$ increased in this case from 0.15 to 0.22 for the sites irradiated with 100 and 500 pulses.

3.4. FTIR analysis

A series of FTIR spectra characterizing a non-irradiated material exposed to a 0.01% H_2O_2 solution for approximately 10 min and the sites irradiated in a 0.01% H_2O_2 solution with

Table 2. XPS concentrations of surface atoms and CA of as-received, etched and KrF laser-processed Si samples with 100 and 500 pulses of 250 mJ cm^{-2}.

	Si (%)	O (%)	C (%)	F (%)	CA
As-received	39.92	54.50	9.58	0	$51 \pm 2.1^\circ$
Freshly etched	83.36	9.75	6.61	0.08	$75 \pm 1.6^\circ$
Non-irradiated exposed to 0.01% H_2O_2	75.73	11.14	13.13	0	$74 \pm 2.2^\circ$
100-pulse irradiated in 0.01% H_2O_2	75.82	12.43	11.75	0	$55.2 \pm 0.8^\circ$
500-pulse irradiated in 0.01% H_2O_2	67.98	23.83	8.19	0	$14.5 \pm 1^\circ$

Table 3. XPS concentrations of surface atoms and CA of as-received, etched and ArF laser-processed Si samples with 100 and 500 pulses of 65 mJ cm^{-2}.

	Si (%)	O (%)	C (%)	F (%)	CA
Non-irradiated exposed to 0.01% H_2O_2	77.05	9.75	12.92	0.28	$73 \pm 0.3^\circ$
100-pulse irradiated in 0.01% H_2O_2	75.95	11.58	12.31	0.11	$63 \pm 1^\circ$
500-pulse irradiated in 0.01% H_2O_2	68.23	25.75	6.01	0.05	$14 \pm 1^\circ$

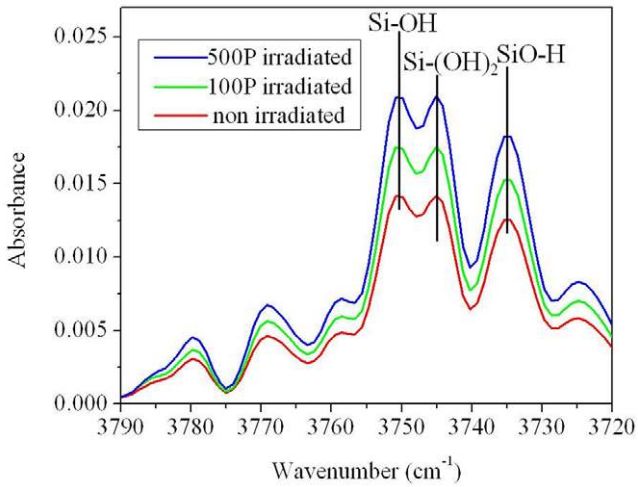

Figure 5. FTIR spectra of non-irradiated site and sites irradiated by KrF laser in 0.01% H_2O_2 solution with 100 pulses (100P) and 500 pulses (500P).

100 and 500 pulses of a KrF laser operating at 250 mJ cm^{-2} are shown in figure 5. The peaks at 3750 cm^{-1} and 3745 cm^{-1} correspond to the Si–OH and Si–$(OH)_2$ vibrational modes, respectively, while the peak at 3735 cm^{-1} is ascribed to the SiO–H stretching vibrational mode (Gupta *et al* 1991, Mawhinney *et al* 1997, Morrow and Gay 1988). It can be seen that the absorbance intensities of these peaks increase with the laser pulse number, thus, indicating a growing concentration of these compounds. This result is consistent with the XPS data discussed above. The insignificant presence of Si-oxides in our samples has been also suggested by our inability to detect an FTIR peak at 1108 cm^{-1} that originates from the Si–O–Si vibrational modes related to oxides created by thermal oxidation of Si in an O_2 environment (Gupta *et al* 1991, Mawhinney *et al* 1997).

3.5. Selective area immobilization of biotinylated nanospheres

Figure 6(*a*) shows a fluorescence image of the Si sample that, after KrF laser irradiation through the maple leaf mask with 400 pulses at 250 mJ cm^{-2} in a 0.01% H_2O_2/H_2O solution, was exposed to a solution of fluorescein-stained nanospheres and, consequently, washed with PBS to remove nanospheres weakly bound to the surface. As expected, a dense accumulation of nanospheres took place on the non-irradiated portion of the sample surface. The morphology of this nanosphere-coated surface is illustrated with an AFM image shown in figure 6(*b*). Although a sharp contrast of the hydrophilic/hydrophobic interface is well depicted in figure 6(*a*), the presence of some defects related to the local increase in the surface hydrophobicity has been illustrated by the nanospheres trapped inside the laser-irradiated zone. The likely source of these defects is the formation of a SiO_2 or SiO_x rich surface in hot spots associated with the formation of bubbles as discussed in section 3.1. A possible strategy towards correction of this problem could include a careful preparation of the Si surface to minimize the presence of surface impurities, and adjusting the conditions of the irradiation, e.g. by reducing the pulse number and/or fluence.

The Si surface selectively patterned with biotin-conjugated nanospheres is important for the fabrication of micro-biosensors and bimolecular electronic devices (Orth *et al* 2003, Stanca *et al* 2005). Our results illustrate the potential of the excimer laser technique for the fabrication of such devices without the need of an ablative patterning that could lead, e.g., to the excessive accumulation of the ablated material in the vicinity of patterned structures.

4. Summary

Modification of the Si surface wettability, initially characterized by CA $\sim$ 75°, has been investigated with a series of samples immersed in low concentrations of H_2O_2/H_2O solutions and irradiated with KrF and ArF lasers. Superhydrophilic surface, characterized by CA $\sim$ 14°, of Si samples immersed in a 0.01% H_2O_2/H_2O solution has been fabricated following the 500-pulse irradiation with 250 mJ cm^{-2} and 65 mJ cm^{-2} pulse fluence of the KrF and ArF laser, respectively. Owing to the relatively low laser pulse fluence, the surface morphology of processed samples remained unaffected as evidenced by the AFM results. XPS and FTIR measurements showed that the formation of a highly hydrophilic surface is associated with the formation of Si–OH

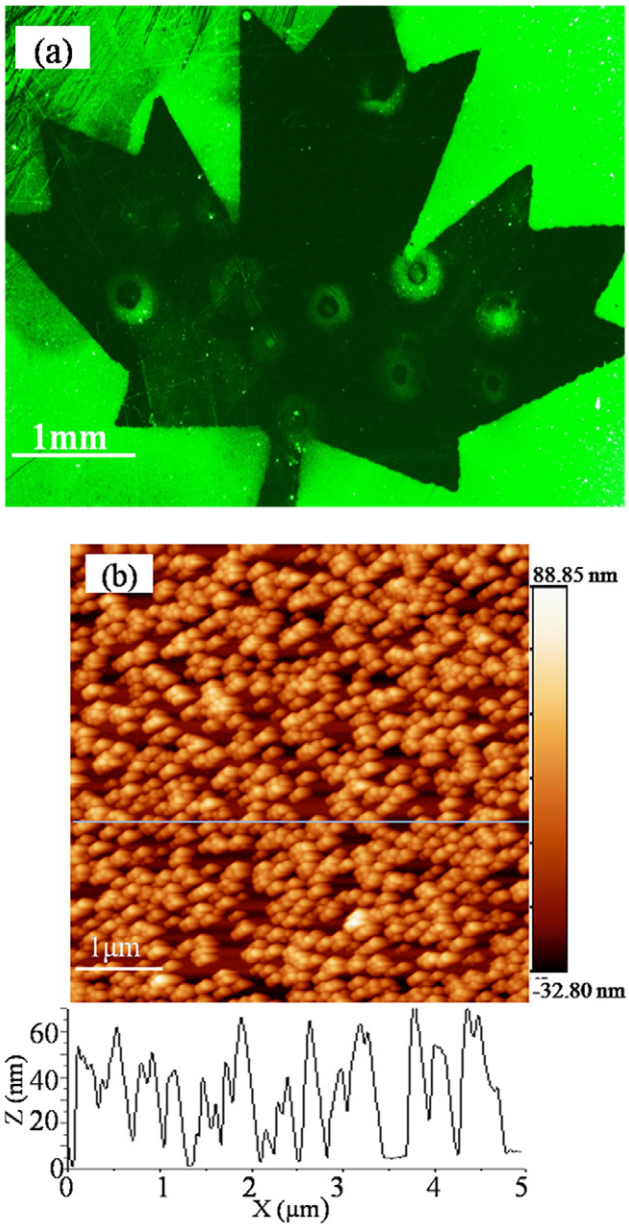

Figure 6. (*a*) Fluorescence image of a sample that, following the irradiation through a maple leaf mask with 400 pulses of a KrF laser at 250 mJ cm^{-2}, was exposed to a solution of fluorescein-stained nanospheres and washed with PBS; (*b*) AFM image of a non-irradiated portion of the sample.

bonds. The laser fabricated hydrophilic surface of Si inhibits the immobilization of biotin-coated nanospheres that naturally stick to the hydrophobic surface of Si. The investigated method of laser-induced modification of the Si surface wettability is compatible with the microfluidic device technology.

Thus, the same approach could be applied to fabricate highly hydrophobic surfaces of Si as we have demonstrated it recently (Liu *et al* 2014). Although we have not carried out repetitive wetting/dewetting experiments in this work, it is reasonable to expect that such a process could be implemented for *in situ* selective area functionalization of Si surfaces investigated, e.g., for the applications involving molecular chemistry research and fabrication of advanced microfluidic devices for (bio)sensing applications.

Acknowledgments

This work was supported by the Natural Science and Engineering Research Council of Canada (Discovery Grant No 122795-2010) and the programme of the Canada Research Chair in Quantum Semiconductors (JJD). The help provided by Dr Kh Moumanus and technical assistance of the Centre de characterization de materiaux (CCM) in collecting XPS data and the Centre de recherche en nanofabrication et en nanocaracterisation (CRN^2) of the Université de Sherbrooke are greatly appreciated. NL acknowledges the Merit Scholarship Programme for Foreign Student, Fonds de recherche du Québec-Nature et technologies, for providing a graduate student scholarship.

References

Aspnes D and Studna A 1983 Dielectric functions and optical parameters of Si, Ge, GaP, GaAs, GaSb, InP, InAs, and InSb from 1.5 to 6.0 eV *Phys. Rev.* B **27** 985–1009

Averill B A and Eldredge P 2007 *Chemistry: Principles, Patterns, and Applications* (New York: Benjamin Cummings)

Bal J K, Kundu S and Hazra S 2010a Hydrophobic to hydrophilic transition of HF-treated Si surface during Langmuir-Blodgett film deposition *Chem. Phys. Lett.* **500** 90–5

Bal J K, Kundu S and Hazra S 2010b Growth and stability of langmuir-blodgett films on OH^-, H^-, or Br^- terminated Si(0 0 1) *Phys. Rev.* B **81** 045404

Baldacchini T, Carey J E, Zhou M and Mazur E 2006 Superhydrophobic surfaces prepared by microstructuring of silicon using a femtosecond laser *Langmuir* **22** 4917–19

Bayiati P, Tserepi A, Petrou P, Kakabakos S, Misiakos K and Gogolides E 2007 Electrowetting on plasma-deposited fluorocarbon hydrophobic films for biofluid transport in microfluidics *J. Appl. Phys.* **101** 103306

Caputo G, Nobile C, Kipp T, Blasi L, Grillo V, Carlino E, Manna L, Cingolani R, Cozzoli P D and Athanassiou A 2008 Reversible wettability changes in colloidal TiO_2 nanorod thin-film coatings under selective UV laser irradiation *J. Phys. Chem.* C **112** 701–14

Chasse M and Ross G 2002 Effect of aging on wettability of silicon surfaces modified by Ar implantation. *J. Appl. Phys.* **92** 5872–7

Chen L, Liberman V, O'Neill J A, Wu Z and Osgood R M 1988 Ultraviolet laser-induced ion emission from silicon *J. Vac. Sci. Technol.* A **6** 1426–7

Chen Y L, Helm C A and Israelachvili J N 1991 Molecular mechanisms associated with adhesion and contact angle hysteresis of monolayer surfaces. *J. Phys. Chem.* **95** 10736–47

Cho S J, An T, Kim J Y, Sung J and Lim G 2011 Superhydrophobic nanostructured silicon surfaces with controllable broadband reflectance *Chem. Commun.* **47** 6108–10

Croiset E, Rice S F and Hanush R G 1997 Hydrogen peroxide decomposition in supercritical water *AIChE J.* **43** 2343–52

Daniel S, Chaudhury M K and Chen J C 2001 Fast drop movements resulting from the phase change on a gradient surface *Science* **291** 633–6

Dubowski J J, Poole P, Sproule G, Marshall G, Moisa S, Lacelle C and Buchanan M 1999 Enhanced quantum-well photoluminescence in InGaAs/InGaAsP heterostructures following excimer-laser-assisted surface processing *Appl. Phys.* A **69** 299–303

Flubacher P, Leadbetter A and Morrison J 1959 The heat capacity of pure silicon and germanium and properties of their vibrational frequency spectra *Phil. Mag.* **4** 273–94

Genest J, Beal R, Aimez V and Dubowski J J 2008 ArF laser-based quantum well intermixing in InGaAs/InGaAsP heterostructures *Appl. Phys. Lett.* **93** 071106

Genest J, Dubowski J J and Aimez V 2007 Suppressed intermixing in InAlGaAs/AlGaAs/GaAs and AlGaAs/GaAs quantum well heterostructures irradiated with a KrF excimer laser *Appl. Phys.* A **89** 423–6

Glassbrenner C J and Slack G A 1964 Thermal conductivity of silicon and germanium from 3 K to the melting point *Phys. Rev.* **134** A1058

Gräf D, Grundner M and Schulz R 1989 Reaction of water with hydrofluoric acid treated silicon(1 1 1) and (1 0 0) surfaces *J. Vac. Sci. Technol.* A **7** 808–13

Grundner M and Jacob H 1986 Investigations on hydrophilic and hydrophobic silicon (1 0 0) wafer surfaces by x-ray photoelectron and high-resolution electron energy loss-spectroscopy *Appl. Phys.* A **39** 73–82

Grunthaner P J, Hecht M H, Grunthaner F J and Johnson N M 1987 The localization and crystallographic dependence of Si suboxide species at the SiO_2/Si interface *J. Appl. Phys.* **61** 629–38

Guo Y, Su S, Wei X, Zhong Y, Su Y, Huang Q, Fan C and He Y 2013 A silicon-based electrochemical sensor for highly sensitive, specific, label-free and real-time DNA detection *Nanotechnology* **24** 444012

Gupta P, Dillon A, Bracker A and George S 1991 FTIR studies of H_2O and D_2O decomposition on porous silicon surfaces *Surf. Sci.* **245** 360–72

Heo J and Kim H J 2007 Effects of annealing condition on low-*k* a-SiOC: H thin films *Electrochem. Solid-State* **10** G11

Hermansson K, Lindberg U, Hok B and Palmskog G 1991 Wetting properties of silicon surfaces *Int. Conf. on Solid-State Sensors and Actuators (San Francisco: IEEE)* pp 193–6

Koehler B G, Mak C H and George S M 1989 Decomposition of H_2O ON Si(1 1 1) 7×7 studied using laser-induced thermal desorption *Surf. Sci.* **221** 565–89

Krupenkin T N, Taylor J A, Schneider T M and Yang S 2004 From rolling ball to complete wetting: the dynamic tuning of liquids on nanostructured surfaces *Langmuir* **20** 3824–7

Li X M, Reinhoudt D and Crego-Calama M 2007 What do we need for a superhydrophobic surface? A review on the recent progress in the preparation of superhydrophobic surfaces *Chem. Soc. Rev.* **36** 1350–68

Lin S-S and Gurol M D 1998 Catalytic decomposition of hydrogen peroxide on iron oxide: kinetics, mechanism, and implications *Environ. Sci. Technol.* **32** 1417–23

Liu N, Hassen W M and Dubowski J J 2014 Excimer laser assisted chemical process for formation of hydrophobic surface of Si (0 0 1) *Appl. Phys.* A in press

Liu N, Moumanis K and Dubowski J J 2012 Self-organized nano-cone arrays in InP/InGaAs/InGaAsP microstructures by irradiation with ArF and KrF excimer lasers *J. Laser Micro/nanoeng.* **7** 130

Liu N, Poulin S and Dubowski J J 2013 Enhanced photoluminescence emission from bandgap shifted InGaAs/InGaAsP/InP microstructures processed with UV laser quantum well intermixing *J. Phys. D: Appl. Phys.* **46** 445103

Lukeš I and Černý R 1992 Study of excimer laser induced melting and solidification of Si by time-resolved reflectivity measurements *Appl. Phys.* A **54** 327–33

Martines E, Seunarine K, Morgan H, Gadegaard N, Wilkinson C D W and Riehle M O 2005 Superhydrophobicity and superhydrophilicity of regular nanopatterns *Nano Lett.* **5** 2097–103

Mawhinney D B, Glass J A Jr and Yates J T 1997 FTIR Study of the oxidation of porous silicon *J. Phys. Chem.* B **101** 1202–6

Miller D, Biesinger M and McIntyre N 2002 Interactions of CO_2 and CO at fractional atmosphere pressures with iron and iron oxide surfaces: one possible mechanism for surface contamination? *Surf. Interface Anal.* **33** 299–305

Mizuno K, Maeda S and Suzuki K-I 1991 Photoelectron emission from silicon wafer surface with adsorption of organic molecules *Anal. Sci.* **7** 345

Morrow B A and Gay I D 1988 Silicon-29 cross-polarization/magic angle spinning NMR evidence for geminal silanols on vacuum-activated aerosil silica *J. Phys. Chem.* **92** 5569–71

Orth R N, Clark T G and Craighead H 2003 Avidin–biotin micropatterning methods for biosensor applications *Biomed. Microdevices* **5** 29–34

Quickenden T I and Irvin J A 1980 The ultraviolet absorption spectrum of liquid water *J. Chem. Phys.* **72** 4416–28

Ranella A, Barberoglou M, Bakogianni S, Fotakis C and Stratakis E 2010 Tuning cell adhesion by controlling the roughness and wettability of 3D micro/nano silicon structures *Acta Biomater.* **6** 2711–20

Rice F O and Reiff O M 1927 The thermal decomposition of hydrogen peroxide *J. Phys. Chem.* **31** 1352–6

Schiffman A, Nelson D D Jr and Nesbitt D 1993 Quantum yields for OH production from 193 and 248 nm photolysis of HNO_3 and H_2O_2 *J. Chem. Phys.* **98** 6935–46

Stanca S E, Ongaro A, Eritja R and Fitzmaurice D 2005 DNA-templated assembly of nanoscale architectures *Nanotechnology* **16** 1905

Sun C, Zhao X W, Han Y H and Gu Z Z 2008 Control of water droplet motion by alteration of roughness gradient on silicon wafer by laser surface treatment *Thin Solid Films* **516** 4059–63

Swift J L and Cramb D T 2008 Nanoparticles as fluorescence labels: is size all that matters? *Biophys. J.* **95** 865–76

Tanaka K, Matsuzaki S and Toyoshima I 1993 Photodecomposition of adsorbed methoxy species by UV light and formaldehyde adsorption on silicon (1 1 1) studied by XPS and UPS *J. Phys. Chem.* B **97** 5673–7

Tsu R, Lubben D, Bramblett T and Greene J 1991 Mechanisms of excimer laser cleaning of air-exposed Si (1 0 0) surfaces studied by Auger electron spectroscopy, electron energy loss spectroscopy, reflection high-energy electron diffraction, and secondary-ion mass spectrometry *J. Vac. Sci. Technol.* A **9** 223–7

Wrobel J M, Moffitt C E, Wieliczka D M, Dubowski J J and Fraser J W 1998 XPS study of XeCl excimer-laser-etched InP *Appl. Surf. Sci.* **127** 805–9

Zorba V, Tzanetakis P, Fotakis C, Spanakis E, Stratakis E, Papazoglou D and Zergioti I 2006 Silicon electron emitters fabricated by ultraviolet laser pulses *Appl. Phys. Lett.* **88** 081103